Modal Interferometer Structures and Splicing Techniques of Fiber Optic Sensor

Nur Hidayah S, Hanim A.R, Hazura H, A.S.M Zain, S.K Idris
Centre for Telecommunication Research and Innovation, Faculty of Electronic and Computer Engineering, Universiti Teknikal Malaysia Melaka, Hang Tuah Jaya, 76100 Durian Tunggal, Melaka, Malaysia
hanim@utem.edu.my

***Abstract*— This paper discusses the properties of modal interference (MI) for fiber optic sensor (FOS). The performances of the devices had been reviewed based on the structures and the splicing techniques. The structures are based on the standard fibers, polarization maintaining fiber (PMF), photonic crystal fiber (PCF) and fiber Bragg grating (FBG). Meanwhile, the splicing techniques can be categorized as the core mode mismatch, offset splicing, waist enlargement and collapse region. This paper also reports the experimental result of core mode mismatch splicing technique of the SMF-SMF and SMF-MMF-SMF. The response of the power received using various operation wavelengths has been examined. At 1530nm operating wavelength, both structures recorded the highest reading of 59.839uW for SMF-MMF and 62.397uw for SMF-MMF-SMF.**

***Index Terms*— Fiber Optic Sensor; Modal Interference; Splicing Technique; Structures.**

I. INTRODUCTION

Optical fiber sensor has received great attention in recent years due to their specialty of sensitivity, size, and immunity to electromagnetic interference in the biological, chemical and environmental industries [1]. Recently, researchers applied the interference phenomenon in many high precision measuring systems, filters, modulators, and sensors [2]-[3].

Interference is an effect of constructive or destructive of electromagnetic wave [4]. Recently, researchers applied the interference phenomenon in many high precision measuring systems and sensors. Optic wave interference is the effect of interference between two optic waves. When using fiber optic as the waveguide, it is known as the fiber optic interferometer (FOI)

FOI is a device that can be used to control and analyze the optical signal [5]. The resultant wave can be analyzed in terms of phase modulation, intensity, power loss, extinction ratio and phase shifting [6]. FOI induced the Michelson interferometer, Fabry-Perot interferometer (FPI), Mach-Zehnder interferometer (MZI) and Sagnac interferometer (SI) for fiber optic sensor (FOS). The applications of FOI as Michelson interferometer for temperature sensor [7], refractive index sensor [8] and for the velocity sensor in [9] have been reported. Meanwhile, the applications of FPI as the refractive index sensor in [8], simultaneous temperature and refractive index sensor in [10] and pressure [11] have been reported. Next, MZI is used for high-temperature sensor [12] and liquid level sensor [13]-[14]. Finally, the application of SI as the refractive index sensor has been reported in [15]. However, the fabrication needs special tools and devices are very fragile.

Modal Interferometer (MI) is another structure of FOI as FOS. The simplicity in signal recovery is the superior property of this structure [16]. MI is a device in which different modes interact with each other and generates an interference pattern that can be in periodic or non-periodic.

There are three sections of the optical fiber MI which are Lead-in, Sensing-area, and Lead-out as shown in Figure 1. Lead-in area allows the optical source to pass through while the Sensing-area responses to the ambient environment. The Sensing Area can be varied in terms of the structures or the types of fiber used. Next is the Lead-out area which acts as a combiner of the received optical signal. The basic physical principle of the device is that optical signal transmitted through the fundamental mode of the Lead-in and coupled to the several modes into the Sensing-area and recoupled to the fundamental mode of the Lead-out section.

This paper describes the differences and the similarities of MI parameters based on the structures, operation principles and the corresponding sensitivity MI as the sensor devices. Furthermore, this paper also reports an experimental result of splicing by using structures SMF-SMF and SMF-MMF-SMF by applying mismatch technique that successfully applied the MI concept.

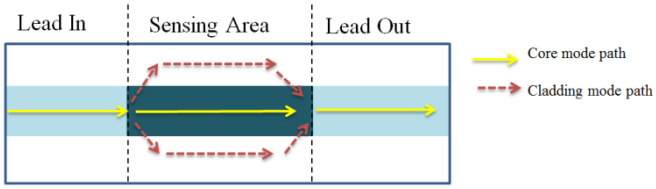

Figure 1: Basic schematic diagram of MI

II. OVERVIEW OF MODAL INTERFEROMETER STRUCTURES

This section describes the structures which have been used as MI as FOI reported by previous research. The structures used such as standard fiber, polarization maintaining fiber (PMF), photonics crystal fiber (PCF) and fiber Bragg grating (FBG) applied to the Sensing-area. In fact, different type of structures will generate different sensitivity response. All the details about the sensitivity are recorded in Table 1.

A. Standard Fibers (SMF/MMF) Based Structures

Single mode fiber (SMF) is a fiber that can carry an optical Single mode fiber (SMF) is a fiber that can carry an optical signal while multimode fiber (MMF) allows multiple modes to propagate along the core. Normally SMF has smaller diameter core compare to the MMF. Jun Su et al. in [17] used

multimode-multimode-multimode (MMF1-MMF2-MMF3) structure fiber for the Sensing-area that cleaved in the SMF and produce three dips at 1555.63nm, 1560.48nm, and 1550.12nm. The sensitivity of the temperature and the refractive index examined by using a linear fitting method through the changes of the dips. Next, Jing li Fan et al. in [18] used a combination of SMF and MMF as the Sensing-area with different structures of fiber to produce a high extinction ratio about -27dB at dip 1573nm. From that, the structure was able to enhance the sensitivity to temperature more than 800℃. Jing-Jing Zhu et al. in [19] used a thin core fiber (TCF) as Sensing-area cleaved into the standard SMF as high temperature optical sensor. The highest temperature can reach 850℃ with a simplest etching process.

B. Polarization Maintaining Fiber (PMF) Based Structures

PMF is also known as high birefringent fibers (HBFs) which linearly polarized planes of light waves [20]. Therefore, the polarization fiber needs a special standard operating procedure in order to maintain the polarization [21]. Hua Ping Gong et al. in [22] reported the waist enlargement splicing PMF between two SMF within specific length the device able simultaneously measured the liquid level, temperature, and refractive index.

C. Photonics Crystal Fiber (PCF) Based Structures

The PCF is also called as the micro-structured fiber. It consists of numerous air holes within a silica host. Jinesh Mathew et al. in [23] spliced PCF as Sensing-area between the SMF to detect dew formation sensor. Other than that, it also responses to the ambient humidity and temperature. Tao Li et al. in [24] cleaved PCF as Sensing-area between the SMF to sense simultaneous strain and temperature. In addition, the PCF was cascaded with long period fiber grating (LPFG) to investigate the different response through the spectral response. Next, Sandipan M. Nalawade et al. in [25] construct a sensor for strain and temperature by splicing PCF as the Sensing-area between SMF and MMF.

D. Fiber Bragg Grating (FBG) Based Structures

FBG was designed by alteration of the wavelength periodically in the fiber. The diffraction is able to confine the optical signal in the core of fiber within the core and cladding [20]. As mention previously in PCF based structures about ref. [24], the PCF was cascaded with FBG to compare the sensitivity response of temperature and strain. The sensor device successfully reduces the complexity of the device. Later, Xiujuan Yu et al. in [26] inscribed FBG in the SMF for simultaneously measured RI and temperature. This device aims to overcome problems in chemical industry, biochemical analysis and also medical diagnostic.

Table 1
Overview of various MI fiber structure for their application, range and the sensitivity.

Sensing-area Structures	Application	Range	Sensitivity	Ref
MM-MM-MM (Standard Fiber)	Refractive Index	1.34-1.39	108.23nm/RIU	[17]
	Temperature	20°C-70°C	0.152nm/°C	
SMF (Standard Fiber)	Refractive Index	1.33-1.37	-64.889nm/RIU	[18]
	Temperature	20°C -80°C	73pm/°C	
TCF(Standard Fiber)	Temperature	0°C -850°C	18.3pm/°C	[19]
PMF	Liquid level	0mm-28mm	-	[22]
	Refractive Index	1.335-1.382	0.516nm/ nm	
	Temperature	25℃-75°C	0.126mm/°C	
PCF	Temperature	20°C -60°C	9.5pm/°C	[23]
	humidity	20%-100%	-	
	Strain	180°	79.83pm/°	[25]
PCF and LPFG	Strain	-	-2.3pm/με (MI) -0.37pm/ με (LPG)	[24]
	Temperature	30°C -100°C	3.2pm/°C (MI) 86.1pm/°C (LPG)	
FBG	Refractive Index	1.33-1.39	-26.22nm/RIU	[26]
	Temperature	20°C -100°C	46.5pm/°C	

III. SPLICING TECHNIQUES

This section describes the splicing techniques to construct structures of Sensing-area for MI. The splicing techniques such as core mode mismatch offset splicing, waist enlargement and collapsed region as reported by previous research. The optical source passed through the Lead-in and approaching Sensing-area and at the Lead-out area will collect a received optical signal from the Sensing-area. Different type of structures caused different pattern propagation of the optical modes.

A. Core Mode Mismatch

Core mode mismatch is formed when the fiber optic core diameter of the Lead-in and the Lead-out are different from the Sensing-area. Jun Su et al. used MMF-MMF-MMF structure for the Sensing-area [17] as shown in Figure 2 MMF1 and MMF3 have the same diameter core of 105/125μm and 5mm length while MMF2 has a core diameter of 50μm/125um with 30mm length. The Lead-in and the Lead-out area used standard SMF-28 while the Sensing-area used TCF with core diameter 1.5 μm with a varied dimension of L about 2cm and 4cm. Meanwhile, MMF1 the optical power coupled to the core and the cladding due to the mode field mismatch and produce multiple core modes and cladding. Then at the MMF3 multiple core modes interfere with cladding modes and core modes of MMF2 due to the phase matching conditions. Next, Jing-Jing Zhu et al. used a TCF structure for the Sensing-area [19] as shown in Figure 3. A high order fiber cladding modes will be excited at the starting edge of Sensing-area. The excited fiber cladding modes will interfere with the core mode due to the relative phase displacement. The output signal is a series of interference signal superposition.

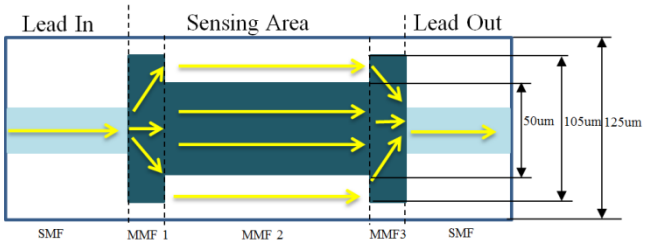

Figure 2: Schematic diagram of a standard fibre

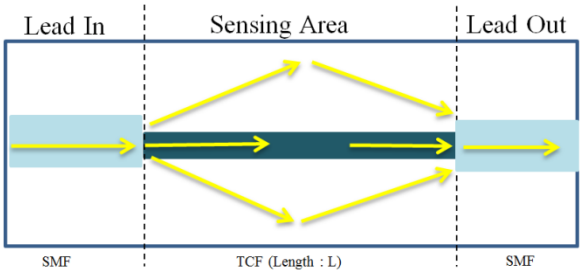

Figure 3: Schematic diagram of TCF

B. Offset Splicing

Offset splicing (OSJ) is formed due to misalignment of the three sections of MI. Tao Li et al. in [26] used FBG as Sensing-area which was spliced between the SMF as shown in Figure 4. The TCF with 9/125µm core diameter was lateral splice offset of 2 µm, 4 µm, and 5.5 µm y-axis. The OSJ1 will excite multiple co-propagating modes, while the OSJ2 will recombine modes. The optical power passed through the FBG will be coupled to the cladding and core mode. The power mode reflected at a particular wavelength in the core mode of FBG. A series of interferences fringes will be produced out of the non-reflected core mode. This is because core mode of FBG and the cladding modes travel through the different optical paths. Subsequently, Jingli Fan et al. cascaded 45mm length SMF and varied length MMF as the Sensing-area by a combination of core mismatch and OSJ techniques in [18] as shown in Figure 5. The varied length of MMF are 1mm, 2mm, and 3mm.The Sensing-area was set up with lateral offset splicing about -4 µm, 4 µm and 2.8284 µm along the x-axis and -4 µm along the y-axis. The sensor depends on the interference between the core mode and the cladding modes in the Sensing-area. The cladding modes are excited due to the lateral mismatch. Optical signal from the SMF Lead-in successfully excites the energy to the sensing SMF, and the optical signal is coupled to the core mode and cladding modes. Then, a part of the core mode and cladding modes will be coupled back to the guided modes of the MMF, before coupled to the fundamental mode of the lead-out SMF

C. Waist Enlargement

Waist enlargement is produced when two tips of fiber merged into one fiber tip by the arc discharge. Hence due to the large overlap and push force between the fiber tips with the fiber waist enlarged [13]. Huaping Gong et al. in [22] spliced SMF with PMF consist two waist that will be enlarged by fiber tapers as shown in Figure 6. Length of PMF used was 35mm with mode field diameter of 10.5 µm.

The waist was enlarged to 165 µm from 125 µm and the taper length of 275 µm. The optical signal propagates in the core through the first waist of enlarged fiber taper, and then the optical signal is coupled to the cladding and core layer of the PMF because of the mismatch diameter. Later at the second waist-enlarged fiber taper, the two optical signal recombine and are partially recoupled back into the core of the Lead-out SMF.

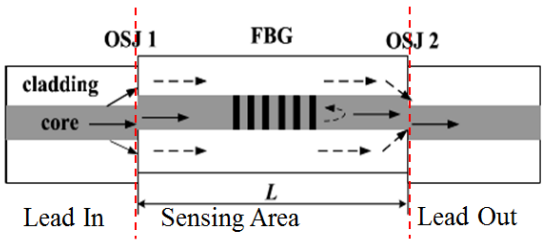

Figure 4: Schematic diagram of OSJ FBG

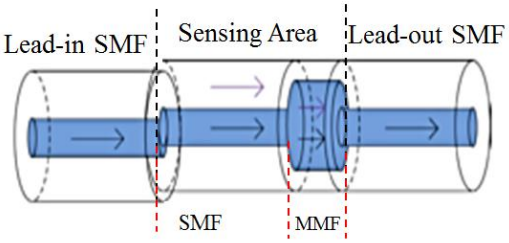

Figure 5: Schematic diagram of mismatch and OSJ

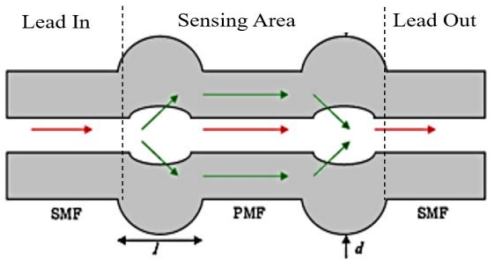

Figure 6: Schematic diagram of waist enlargement

D. Collapse Region

Collapse region happens during splicing of microstructure fiber which is the PCF. The air holes of the PCF at the splicing regions are fully collapsed. Figure 7 shows the excitation and recombination mode in the hole of the collapsed region based on Tao Li et al in [24]. It used standard SMF-28 with 17mm length solid core PCF (LMA10) as the Sensing-area. The modes propagate through the PCF until reaching the cleaved end and produce reflected optical signal. When the reflected modes re-enter the collapsed region the modes will further diffract. The cladding modes and core mode generates a phase difference when they are propagating along the PCF. The cladding modes of the PCF will couple back into the core of the Lead-out area

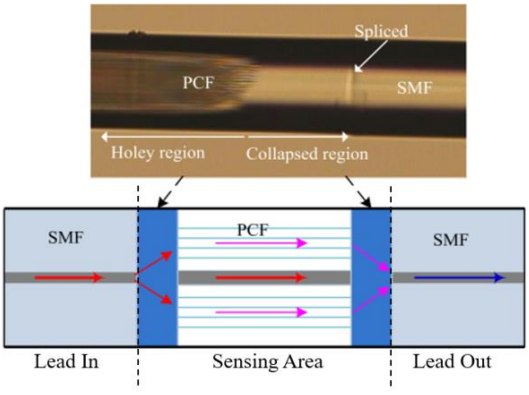

Figure 7: Schematic diagram of collapse region

IV. SPLICING RESULT

The response of the power received using various operation wavelength have been examined. Figure 8 shows the schematic diagram splicing between SMF-SMF with L_1 and L_2 are 1m length. Figure 9 shows the schematic diagram for SMF-MMF-SMF with L_3 and L_4 are 2m and 0.14m respectively.

This paper used standard SMF-28 and graded MMF with 62.5/125 µm. This paper used WSL-100 and OSA MS9740A as tuneable wavelength source and the spectrum analyzer. The operating wavelength was set in the range of 1530nm to 1600nm with an interval of 10nm. This experiment used 5mw as the input power supply. Figure 10 shows the power output graph displayed in µW for each configuration. Then the graphs pattern are almost the same but slightly different at 1590nm. In addition the SMF-SMF structure shows lowest transmission power output compared to SMF-MMF-SMF. This is due to the property of MMF that can carry more signals compared to the SMF. It can be seen that at 1530nm operating wavelength both structures of SMF-SMF and SMF-MMF-SMF show the highest reading with 59.839uW and 62.397uw respectively.

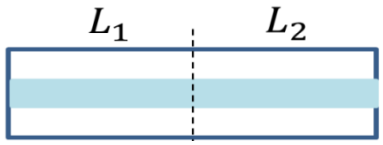

Figure 8: Schematic diagram splicing of SMF-SMF structure

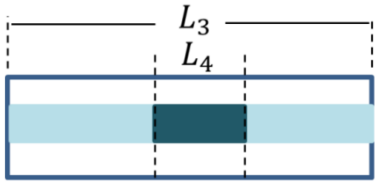

Figure 9: Schematic diagram splicing of SMF-MMF-SMF structure

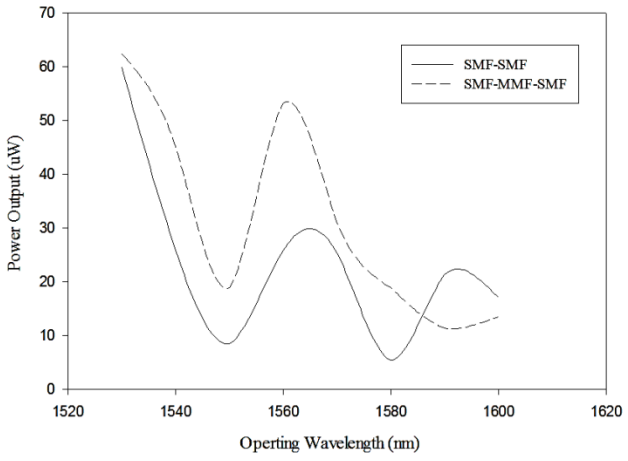

Figure 10: Transmission power output

V. CONCLUSION

This paper has discussed the MI device in terms of the structure and the splicing techniques. A different configuration of the MI device depends on the applications. Meanwhile, there were a variety of techniques applied in order to construct the MI device sensor, but core mode mismatch structure is the most effective splicing technique due to the flexibility of the splicer machine.

ACKNOWLEDGMENT

This paper is supported under grants of UTeM Zamalah Scheme, RAGS/1/2014/TK03/FKEKK/B00060 and F00299-RACE/F3/TK3/FKEKK.

REFERENCES

[1] G. Orellana and D. Haigh, "New Trends in Fiber-Optic Chemical and Biological Sensors," *Curr. Anal. Chem.*, vol. 4, no. 4, pp. 273–295, 2008.

[2] H. Haroon, M. Bidin, H. Abdul, P. S, and N. Arsad, "Impact of Coupled Resonator Geometry on Silicon-on Insulator Wavelength Filter Characteristics," pp. 380–382, 2011.

[3] H. Hazura, S. K. Idris, A. S. M. Zain, F. Salehuddin, and P. S. Menon, "Modeling Mach Zehnder Interferometer (MZI) Modulator on Silicon-On-Insulator (SOI)," vol. 8, no. 1, pp. 121–124, 2016.

[4] F. L. Pedrotti, L. M. Pedrotti, and L. S. Pedrotti, *Introduction to Optics*, Third. .

[5] D. Krohn, T. MacDougall, and M. Alexis, *Fiber Optic Sensors Funfamentals and Applications*, Fourth. Bellingam, Washington USA: SPIE PRESS, 2014.

[6] K. Abe, Y. Lacroix, L. Bonnell, and Z. Jakubczyk, "Modal Interference in a Short Fiber Section: Fiber Length, Splice Loss, Cutoff, and Wavelength Dependences," *J. Light. Technol.*, vol. 10, no. 4, pp. 401–406, 1992.

[7] Y. Zhang *et al.*, "A novel Michelson Fabry-Perot hybrid interference sensor based on the micro-structured fiber," *Opt. Commun.*, vol. 374, pp. 58–63, 2016.

[8] J. R. Guzmán-Sepúlveda, R. Guzmán-Cabrera, M. Torres-Cisneros, J. J. Sánchez-Mondragón, and D. A. May-Arrioja, "A highly sensitive fiber optic sensor based on two-core fiber for refractive index measurement.," *Sensors (Basel).*, vol. 13, no. 10, pp. 14200–14213, 2013.

[9] L. Yuan, J. Yang, and Z. Liu, "A compact fiber-optic flow velocity sensor based on a twin-core fiber Michelson interferometer," *IEEE Sens. J.*, vol. 8, no. 7, pp. 1114–1117, 2008.

[10] D. Wu, T. Zhu, Guo-Yin Wang, Jian-Yu Fu, X.-G. Lin, and G.-L. Gou, "Intrinsic fiber-optic Fabry-Perot interferometer based on arc discharge and single-mode fiber.," *Appl. Opt.*, vol. 52, no. 12, pp. 2670–5, 2013.

[11] Q. Yu and X. Zhou, "Pressure sensor based on the fiber-optic extrinsic fabry-perot interferometer," *Photonic Sensors*, vol. 1, no. 1, pp. 72–83, 2011.

[12] L. V. Nguyen, D. Hwang, S. Moon, D. S. Moon, and Y. Chung, "High temperature fiber sensor with high sensitivity based on core diameter mismatch.," *Opt. Express*, vol. 16, no. 15, pp. 11369–11375, 2008.

[13] Y. Geng, X. Li, X. Tan, Y. Deng, and Y. Yu, "High-sensitivity Mach-Zehnder interferometric temperature fiber sensor based on a Waist-Enlarged fusion bitaper," *IEEE Sens. J.*, vol. 11, no. 11, pp. 2891–2894, 2011.

[14] H. A. Razak, N. H. Sulaiman, H. Haroon, and A. S. Mohd Zain, "A fiber optic sensor based on Mach-Zehnder interferometer structure for food composition detection," *Microw. Opt. Technol. Lett.*, vol. 60, no. 4, pp. 920–925, 2018.

[15] B. Dong, J. Hao, C. Y. Liaw, and Z. Xu, "Cladding-mode resonance in polarization-maintaining photonic-crystal-fiber- based sagnac interferometer and its application for fiber sensor," *J. Light. Technol.*, vol. 29, no. 12, pp. 1759–1763, 2011.

[16] B. T. M. K. T. V. Grarttan, "Optical Fiber Sensor Technology-Aplication and System," vol. 3–1587, pp. 350–361, 1999.

[17] W. Z. Jun Su, Zhengrong Tong, Ye Cao, "High sensitivity multimode-multimode-multimode structure fiber sensor based on modal interference," *Opt. Commun.*, vol. 315, pp. 112–115, 2014.

[18] Jingli Fan, Jisngshan Zhang, Ping LuMing Tian, Jun Xu, and D. Liu, "A single-mode fiber sensor based on core-offset inter-modal interferometer," *Opt. Commun.*, vol. 320, pp. 33–37, 2014.

[19] J. J. Zhu, A. P. Zhang, T. H. Xia, S. He, and W. Xue, "Fiber-optic high-temperature sensor based on thin-core fiber modal interferometer," *IEEE Sens. J.*, vol. 10, no. 9, pp. 1415–1418, 2010.

[20] I. Padron, *Interferometry-Research and Applications in Science and Technology*. 2016.

[21] L. Thévenaz, *Advanced Fiber Optics*. 2011.

[22] H. Gong, H. Song, S. Zhang, K. Ni, and X. Dong, "An optical liquid level sensor based on polarization-maintaining fiber modal interferometer," *Sensors Actuators, A Phys.*, vol. 205, pp. 204–207, 2014.

[23] and G. F. Jinesh Mathew, Yuliya Semenova, "Photonic crystal fiber

interferometer for dew detection," *J. Light. Technol.*, vol. 30, no. 8, pp. 1150–1155, 2012.

[24] Tao Li, X. Donga, C. C. Chanb, L. Hua, and W. Qian, "Simultaneous strain and temperature measurement based on a photonic crystal fiber modal-interference interacting with a long period fiber grating," *Opt. Commun.*, vol. 285, no. 24, pp. 4874–4877, 2012.

[25] S. M. Nalawade, S. S. Harnol, and H. V. Thakur, "Temperature and strain independent modal interferometric torsion sensor using photonic crystal fiber," *IEEE Sens. J.*, vol. 12, no. 8, pp. 2614–2615, 2012.

[26] X. Yu, X. Chen, D. Bu, J. Zhang, and S. Liu, "In-fiber modal interferometer for simultaneous measurement of refractive index and temperature," *IEEE Photonics Technol. Lett.*, vol. 28, no. 2, pp. 189–192, 2016.